

## ELECTRO-THERMOMECHANICAL PROPERTIES OF SUPERELASTICITY IN SINGLE CRYSTALS SHAPE MEMORY ALLOYS

Cezar Henrique Gonzalez, [gonzalez@ufpe.br](mailto:gonzalez@ufpe.br)

Carlos Augusto do Nascimento Oliveira, [cano.oliveira@gmail.com](mailto:cano.oliveira@gmail.com)

Euclides Apolinário Cabral de Pina, [euclidescvang@yahoo.com.br](mailto:euclidescvang@yahoo.com.br)

Severino Leopoldino Urtiga Filho, [urtiga@ufpe.br](mailto:urtiga@ufpe.br)

Oscar Olímpio de Araújo Filho, [oscaroaf98@hotmail.com](mailto:oscaroaf98@hotmail.com)

Universidade Federal de Pernambuco – Centro de Tecnologia e Geociências – Departamento de Engenharia Mecânica, Av. Acadêmico Hélio Ramos, s/n, Cidade Universitária, 50740-530, Recife - PE

Carlos José de Araújo, [carlos@dem.ufcg.edu.br](mailto:carlos@dem.ufcg.edu.br)

Universidade Federal de Campina Grande, Departamento de Engenharia Mecânica, Av. Aprígio Veloso, 882, Caixa Postal: 10069, Campina Grande - PB, CEP 58109-970, Brasil

**Abstract.** *In this work, superelastic behaviour of single crystals shape memory alloys has been investigated by the electric resistivity (ER) measure technique coupled simultaneously during traction tests. Samples in austenitic phase were submitted to stress induced martensite (SIM) under several conditions such as: different temperatures, different deformation rates, throughout successive martensitic transformations and different crystallographic orientation axes. ER versus deformation curves presented a linear relation without hysteresis and independence on temperature. In the case on the increasing of deformation rates, these curves show a little hysteresis due to adiabatic transformations. For samples submitted to successive transformations, ER curves showed changes with induced martensite types. In samples of the same alloy with different crystallographic orientations was observed that single variant martensite nucleation presented distinct values, this characterizes martensite electric resistivity anisotropy.*

**Keywords:** *Thermoelasticity, Smart Materials, Shape Memory Effects, Electro-thermomechanical Properties, Superelasticity.*

### 1. INTRODUCTION

Thermoelastic properties of the martensitic transformation are manifested through some phenomena: one-way shape memory effect, two-way shape memory effect and pseudo-elasticity, which can be divided in superelasticity and rubber-like behaviour<sup>1</sup>. Superelasticity is characterized by the martensite induction due to the application of an external mechanical load right above the temperature  $A_F$  (austenitic finish transformation temperature) from what the austenitic phase is stable. Martensitic transformation occurs because  $M_S$  (martensitic start transformation temperature) increases since that external stress applied makes unstable the balance in energy among austenitic and martensitic phases (Wyman et al, 1998, Otsuka et al, 1986).

Initially in the superelastic curves, the austenite is elasticity deformed and later with the increase in stress the sample reaches critical stress that induces the formation of the martensite plates. Stress favours the growing of certain variant until all the sample is in the martensitic state. This transformation is accompanied by a pseudo-plastic deformation which can attain 6% in polycrystalline and 18% in single crystalline materials. In this last material frequently occurs successive martensitic transformations<sup>2</sup>. In these tests, stress-strain curves ( $\sigma$ - $\epsilon$ ) show that the transformation occurs at practically constant stress, mainly in single crystals. Metastable condition is suppressed when the external load is removed, changing to stable austenitic phase again and the sample recover all produced deformation used to nucleate the martensite crystal, generating a hysteresis loop in the  $\sigma$ - $\epsilon$  curve.

Large deformation obtained and its reversible character presents large interests to technological applications. This phenomenon is much applied in orthodontia, mechatronics, robotics and others. In technical applications and numeric simulations of this effect is necessary to know the shape of the stress versus superelastic deformation. There are several features which can influence this curve as follow: temperature, deformation rate, heat treatments, martensite structure type (3R, 6R, 9R, 18R, 2H or 4H), successive martensitic transformation, crystallographic orientation (case of single crystals) and texture (polycrystal cases) (Otsuka et al, 1998, Amengual et al, 1990, Brown, 1981). This implies in several consequences in superelastic curves to nucleate the martensite crystal.

In this work, Cu-based (Cu-Zn-Al e Cu-Al-Be) single crystals shape memory alloys were submitted to different conditions of superelastic tests: different temperatures, different deformation rates, successive martensitic transformation and crystallographic orientations. The electro-thermomechanical properties obtained on superelastic and in electric resistivity curves as a function of strain were evaluated taking as regard the martensitic transformation theory and the features which affect the superelastic behaviour mentioned in the previous section.

## 2. MATERIALS AND METHODS

Cu-based shape memory alloys were obtained in an induction furnace at 1200°C and single crystals growing were performed by a modified Bridgman method. Alloys references with their chemical compositions, critical temperatures and transformation enthalpies are presented in table 1. Tensile samples were manufactured by a spark-cutting technique in the following dimensions: useful length = 10 mm, width = 4 mm and thickness = 1.2 mm. The samples were submitted to heat treatment of solubilization at 850°C during 15 minutes, quenched in water at 25°C and annealing in water at 100°C for 1 hour, intending the annihilation of the supersaturated vacancies introduced by quenching and to stabilize austenitic phase ( $\beta_1$ ).

Table 1. Alloys Characteristics

Reference	Chemical Composition (mass %)				Critical Transformations Temperatures (°C)				Entalphy (J/g)
	Cu	Al	Be	Zn	$M_S$	$M_F$	$A_S$	$A_F$	
<b>CAB5</b>	87.58	12.00	0.42	-	9	-11	2	18	7
<b>CAB10</b>	87.53	12.00	0.47	-	10	-5	6	21	7
<b>CAB12</b>	87.52	12.00	0.48	-	2	-13	-1	16	7
<b>CZA3</b>	76.2	15.80	-	8.00	-4	-16	-6	2	6.5
<b>CZA10</b>	76.60	15.40	-	8.00	38	32	40	42	9
<b>CZA11</b>	76.60	15.40	-	8.00	35	28	37	41	9

Tests were realized in a servo-pneumatic stress test machine manufactured and specially designed to study and evaluate shape memory phenomena<sup>4</sup>. Tests were conducted at a constant deformation rate of 0.2% min<sup>-1</sup> and in these tests performed to evaluate the influence of the deformation rate were used 0.6 and 1.0 % min<sup>-1</sup>. Sample temperatures were maintained constant and homogenous by a control system with a maximum variation of  $\pm 0.1^\circ\text{C}$ .

Electric resistivity (ER) measurements were carried out by conventional four point terminals method coupled tensile tests. In this method, a well-stabilized current passes across the sample and potential difference ( $\Delta V$ ) is measured thought the useful length. Gonzalez *et al* present details of the coupling ER measurements in tensile tests experimental procedures<sup>5</sup>. Equation 1 represents electric resistivity changes where  $R_\epsilon$  and  $\rho_\epsilon$  are respectively the electrical resistance and electrical resistivity for a given strain,  $R_{\epsilon_0}$  and  $\rho_{\epsilon_0}$  corresponding to the properties just before test ( $\epsilon$  null at test temperature). This equation is applied to eliminate contribution of geometric changes promoted by sample strain, since thermoelastic martensitic transformation is considered a process at constant volume.

$$\frac{\Delta\rho_\epsilon}{\rho_{\epsilon_0}} = \frac{\Delta R_\epsilon}{R_{\epsilon_0}} - 2 \cdot \epsilon \quad (1)$$

Testing samples of the different crystallographic tension axes were produced by cutting in a spark-machine singles crystal of Cu-Zn-Al with angles of 4° (CZA10 alloy) among each sample and of 9° for Cu-Al-Be (CAB12 alloy). Some tensile samples were observed *in situ* by means of optical microscopy technique and an attachment apparatus for application of stress. Microstructures were captured utilizing polarized light and Normanski contrast interface.

## 3. RESULTS AND DISCUSSION

In this work, all tests were conducted with samples in the austenitic phase (test temperature  $> A_F$ ). Results of electro-thermomechanical properties in the superelastic state are presented for four test conditions: influence of temperature, deformation rate, successive martensitic transformation and different crystallographic orientations.

### 3.1 Test temperature influence

Figure 1 presents electrical resistivity coupled with stress-strain measurement on CAB10 single crystal at temperatures 40, 50, 60, 70 and 80°C. Stress curves show martensite induction after to attain critical stress. Transformation occurs by interface austenite/martensite formation which grows progressively with the strain at practically constant stress. When martensitic single crystal is completely formed, the stress begins to increase quickly. In the crystal tested, the transformation strain was nearly 7.8%. When the load is relaxed, starts reverse martensitic transformation which in the absence of load the austenitic phase is more stable. In this way, sample starts recovering its original shape during reverse transformation (martensite => austenite).

A hysteresis is observed in strain-strain curves of about 11 MPa. This hysteresis should be zero in theory but several factors can influence its formation as follow: resistances to nucleation or moving austenite/martensite interfaces, local relaxation of elastic deformation energy, martensite stabilization processes and thermodynamic character of the direct and reverse transformations once first is exothermic and second is endothermic (Lovey et al, 1992, Gonzalez et al, 2004). For temperature tests, hystereses are almost the same since strain rate was maintained constant and dissipation environment was the same for all tests.

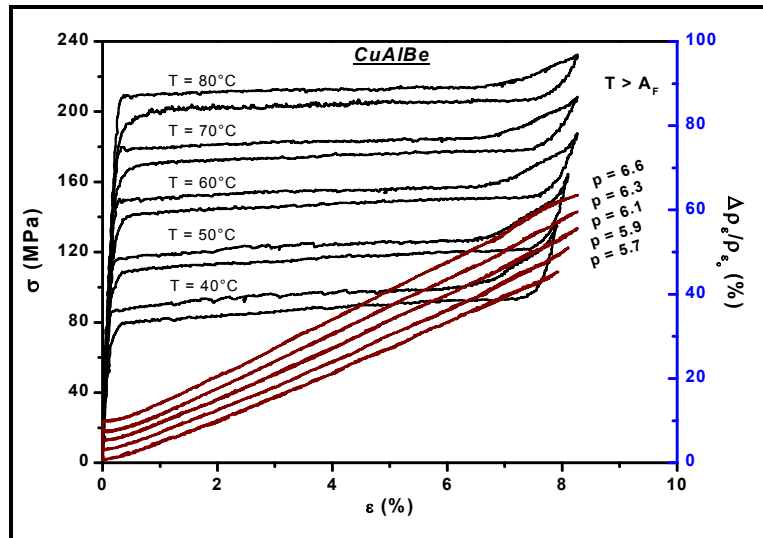


Figure 1. Effect of temperature in the electro-thermomechanical properties of the superelastic tests (CAB10).

Critical stress of martensite induction increases progressively and linearly with the increase in temperature as foreseen by Clausius-Clapeyron thermodynamic relation<sup>2</sup>. In figure 2 is shown a phase diagram stress versus temperature type ( $\sigma$ -T), where the two straight lines represent the critical stress of direct (full line) and reverse (dot line) transformations. These straight lines have a rate of 2.9 MPa/°C representing the thermodynamic relation among the two phases (austenite and martensite). The  $M_S$  and  $A_S$  samples temperatures without application of external stress can be determined by extending of two straight lines. These temperatures are much closed with those determined by DSC values.

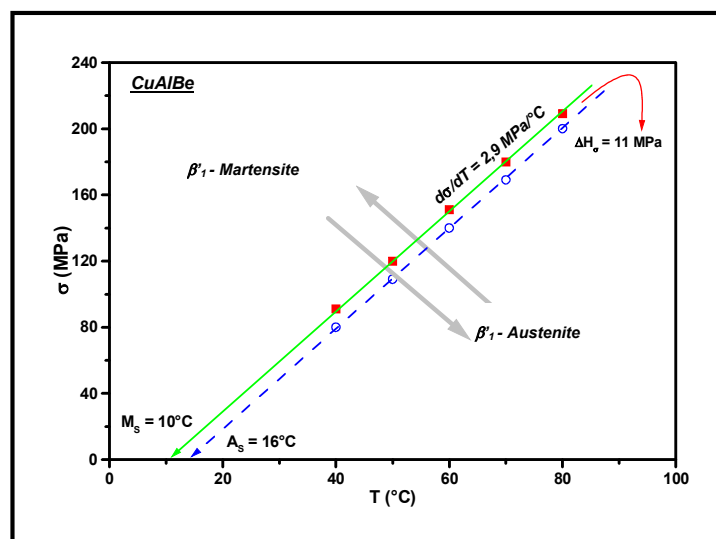


Figure 2. Phase diagram of  $\sigma$ -T type for CAB10 sample (full and dot line – direct and reverse transformation, respectively).

Electrical resistivity change versus strain ( $\Delta\rho_e/\rho_{e0} - \epsilon$ ) curves superimpose one another, so here they were shifted in y axis to be better visualized. ER curves in the elastic region are practically constant. From critical stress for oriented martensite needles induction, they present a rate which increase linearly with strain and therefore with martensite quantity formed. ER change measure ( $\Delta\rho_e/\rho_{e0}$ ) for martensite oriented crystal formation is about 43%, independent on

temperature. These curves don't show formation of hysteresis among direct and reverse transformation. Electrical behaviour seems to be less sensible to influences generated by thermodynamic character of transformation.

### 3.2. Deformation rate influence

Figure 3 presents superelastic tests carried out in a sample of CZA11 alloy in a constant temperature of 60°C, using three strain rates: 0.2, 0.6 e 1.0%.min<sup>-1</sup>. One superelastic cycle with rate of 0.2%.min<sup>-1</sup> was conducted between each test to suppress eventual interactions among the different tests.

Differences among rates adopted in these tests aren't significant but enough to make evidence the increase in the stress hysteresis ( $\sigma$ - $\epsilon$  curves) with increase of strain rate, but martensite induction critical stress is practically unchangeable. ER change to attain the oriented martensite single crystal almost shows a measure of about 41%, independent of strain rate. ER curves begin to appear very slim hysteresis loop from strain rate of 0.6%.min<sup>-1</sup>.

Transformation is considered isothermal at low strain rates and adiabatic to higher rates (Brown, 1981). Stress hysteresis increase with strain rate due to mainly thermal effect generated in the neighbourhood of sample. This happens due to exothermic reaction during direct martensitic transformation (Delaey et al, 1987, Brown, 1981). The heat generated can't be wasted quickly in the neighbourhood of sample, even for sample immersed in an oil bath temperature control. During unloading occurs reverse transformation (austenitic transformation) that has endothermic character, cooling the sample. Thus stress and ER hysteresis tends to increase due to these characteristics of the direct and reverse transformations. During direct transformation, sample heats consequently increasing stress induction (Clausius-Clapeyron relation). During unloading, reverse transformation occurs promoting the decrease in stress. This effect is more important when tests are realized at room environment<sup>9</sup>.

For ER curve at rate of 1.0%.min<sup>-1</sup>, hysteresis loop presents a maximum width of about 0.6% corresponding to a thermal variation of about 2°C. This estimate was done from austenitic phase resistivity changes results as a function of temperature by comparing with the measures obtained in literature<sup>9</sup>.

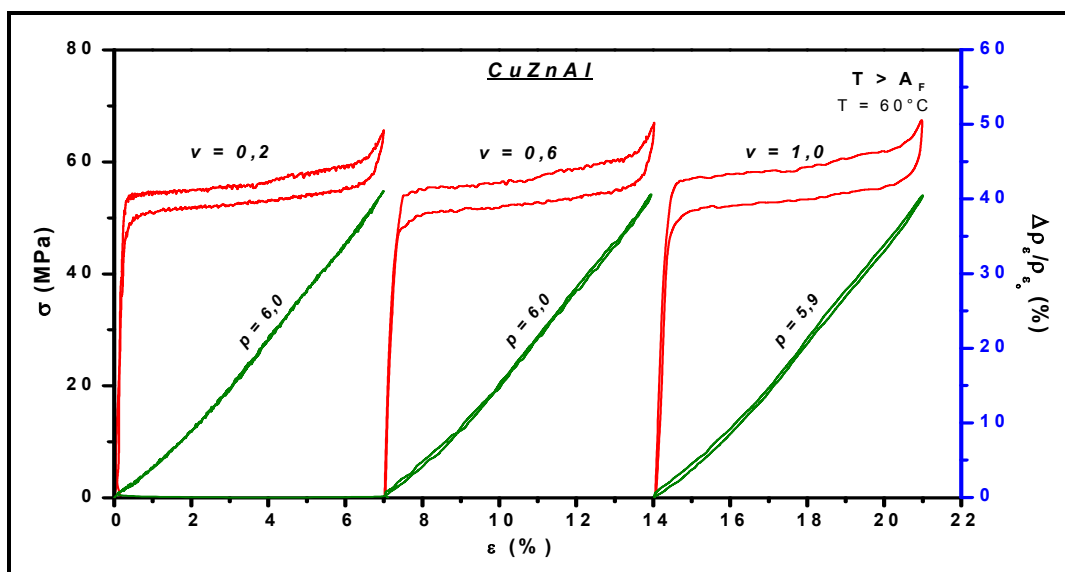


Figure 3. Strain rate influence in the superelastic electro-mechanical curves of CZA11 sample for strain rates: 0.2, 0.6 and 1.0%.min<sup>-1</sup>.

### 3.3. Successive martensitic transformations

Figure 4 shows electro-mechanical test results obtained in CAB5 alloy sample, presenting two successive martensitic transformations. The OA interval corresponds to austenite elastic strain domain. In AB interval occurs nucleation of the single variant  $\beta_1'$  martensite, characterized by forming a plateau stress. The ER curve in this interval presents a linear variation with slope of 3.3 ( $p_1$ ) and a change of 31% for former single variant crystal martensite. In the following interval (BC) occurs  $\beta_1'$  martensite elastic deformation and  $\alpha_1'$  martensite nucleation. This process occurs by the shearing system accompanied by a partial consecutive nucleation and their subsequent expansion (Delaey et al, 1987, Brown, 1981). The increase in stress is accompanied by an ER change of about 6% and slope of 4.7. In the CD interval is shown the induction of successive martensite transformation ( $\beta_1' \leftrightarrow \alpha_1'$ ). This is characterized by formation of a second plateau in stress curve ( $\sigma \approx 275$ MPa). Maximum theoretical transformation strain for the two successive transformations in Cu-Al-Be alloy ( $\beta_1 \leftrightarrow \beta_1' \leftrightarrow \alpha_1'$ ) is about 19.5%<sup>10</sup>. The test was interrupted at a strain of 14% in order to avoid the fracture of the sample. In this interval, ER curve behaviour is altered in comparison with previous intervals, showing ER change of 5% and a completely different slope ( $p_3 = 1.4$ ).



Sample is unloaded in the D point, beginning reverse transformations (DF interval -  $\alpha_1' + \beta_1' \Rightarrow \beta_1$ ). Large stress hysteresis is a consequence of the phase energies differences indicating the coexistence of two martensites during unloading (Otsuka et al, 1986). ER curve presents also a hysteresis in this interval, probably related to latent heat variations during phase transformations.

Figure 5 shows results of test in a Cu-Zn-Al alloy (CZA3) realized at  $-20^\circ\text{C}$ , below of  $M_F$  temperature. In this case, martensitic phase ( $\beta_1'$  martensite) was initially deformed, differently of previous tests. During AB interval occurs  $\beta_1'$  martensite variants reorientation process where variants that has the highest Schmidt factor increase in the expense of other variants<sup>5</sup>. In the B point was formed a variant single martensite. If test was stopped in B point, during unloading will presents a residual strain. This can to be recovered by heating. Elastic deformation of the single crystal martensite is showed in the BC interval. From C point was started successive martensitic transformation  $\beta_1' \Leftrightarrow \alpha_1'$ . Tensile sample was unloading in the D point and reverse transformation ( $\alpha_1' \Leftrightarrow \beta_1'$ ) began. Final point is undefined because in the stress curve they can to be E or F point. Even in the G point ( $\sigma = 0$  MPa) the sample can probably present a mixed state of two martensite types.

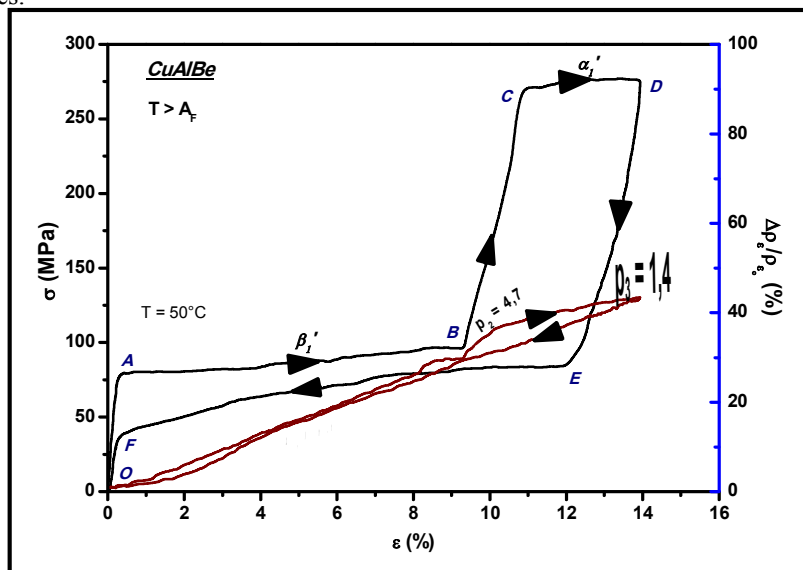


Figure 4. Electro-mechanical curves of successive martensitic transformation in the CAB5 sample.

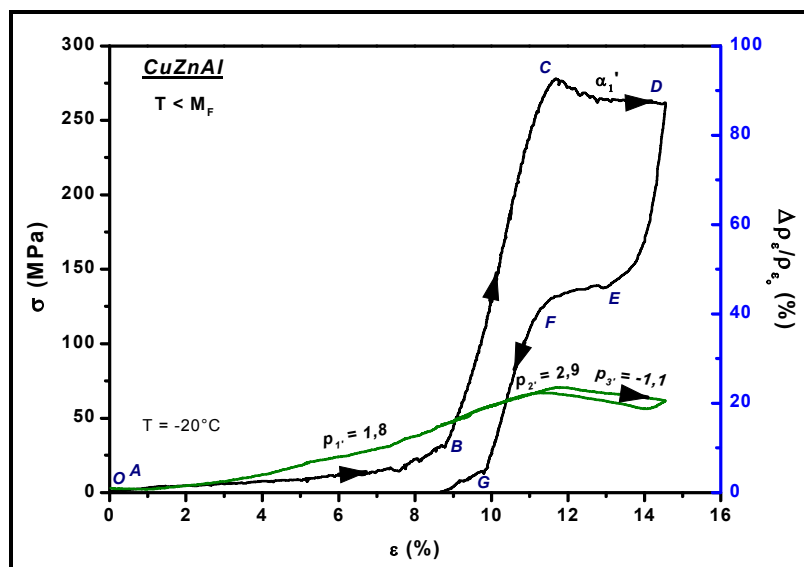


Figure 5. Electro-mechanical curves of successive martensitic transformation in the CZA3 sample.

ER curve shows how resistivity measure changes during martensite variants reorientation process (B point =  $\rho_e/\rho_{e0} \approx 17\%$ ) which is always smaller than the value obtained to stress induced martensite (from figure 1, 3 and 4,  $\rho_e/\rho_{e0}$  varies among 30-40%). This comparison is important because in both process the result is a single variant martensite crystal. This may evidence electrical anisotropy of martensite structure. In the BC interval, ER curve slope changes indicating

the presence of other process (elastic strain of single martensite). In the following interval (CD), a new modification in ER curve (and in the slope) is showed due to successive martensitic transformation. ER measure decreases during  $\alpha_1'$  martensite growing because its value is inferior when compared with polyvariant martensite reference value ( $\beta_1'$  without loading -  $\rho_{e0}$ ). Comparatively from previous test, ER change measure for the  $\alpha_1'$  martensite induction which is smaller than that of  $\beta_1'$  martensite. This evidences the sensibility of ER measuring to detect the phase transformations. In the stress curve finish of the reverse transformation ( $\alpha_1' \Leftrightarrow \beta_1'$ ) isn't conclusive (E, F or G point), but in ER curve it is closed for F point because from this point the direct and reverse transformation ER curves are superpose. This conclusion is due to the ER measure to be more sensible of than mechanical technique.

### 3.4. Crystallographic orientations different influence

Figures 6 and 7 show single crystals superelastic tests obtained in the CZA10 and CAB12 samples at 80 and 40°C, respectively. Three tensile samples of each alloy were prepared with orientations crystallographic of the tensile axis. For Cu-Zn-Al alloy, the difference between each sample was 4 degrees and 9 degrees for Cu-Al-Be alloy. Changes in the crystallographic orientation of the tensile axis influences critical stress of the martensite induction, constant level of stress for martensite formation (plateau without inclination in the stress curve) and maximum transformation strain to obtain the martensite single crystal (Otsuka et al, 1986, Gonzalez et al, 2004). In the superelastic test, only one of the 24 martensite variants is favoured by the crystallographic relations with direction tensile axis. Single variant induced will be the one which leads to the highest Schmidt factor (Gonzalez et al, 2004).

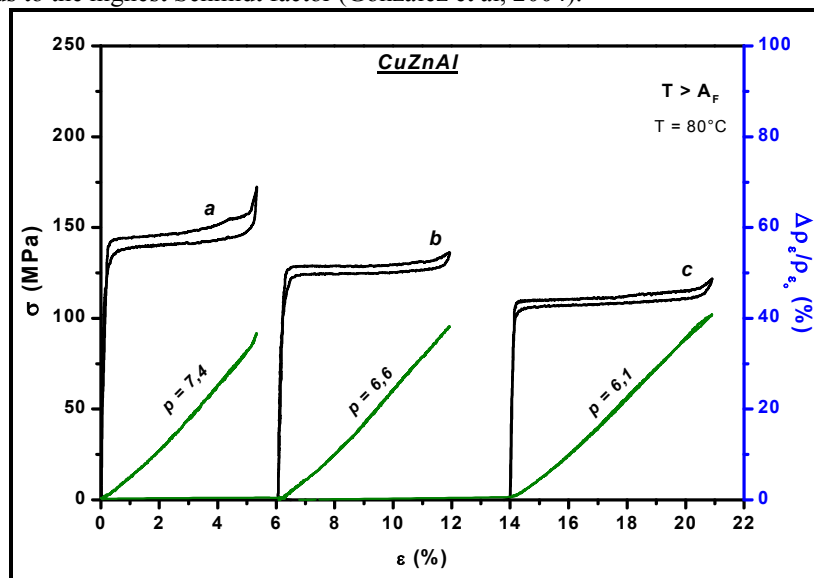


Figure 6. Superelastic tests in the CZA10 tensile samples with different crystallographic orientations (Cu-Zn-Al alloy).

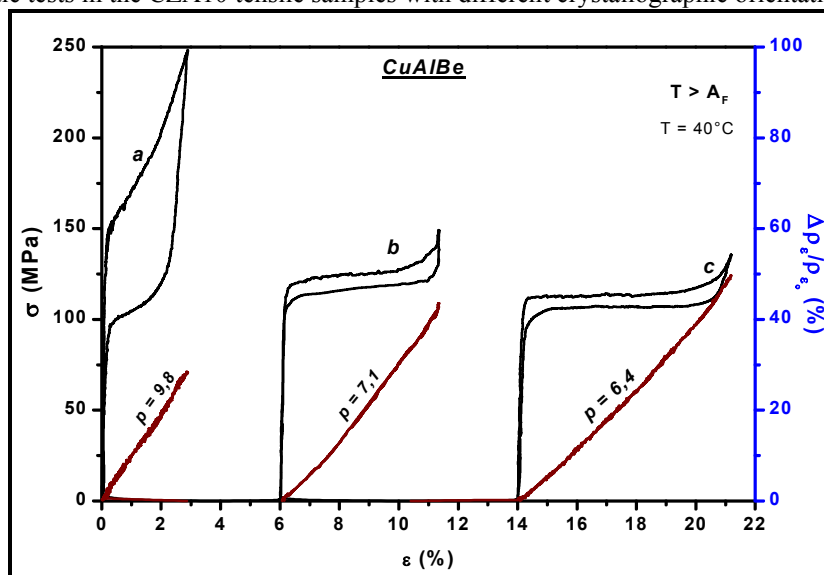


Figure 7. Superelastic tests in the CAB12 tensile samples with different crystallographic orientations (Cu-Al-Be alloy).

In the figure 8 is shown micrographs of the b and c CAB12 tensile samples by means of optical microscopy where only one variant was induced in each sample. Crystallographic orientations of the martensite variant activated in each sample are different in relation to the tensile axis. This is evident because each martensite plates in each sample (some alloy) has different angles with the tensile axis.

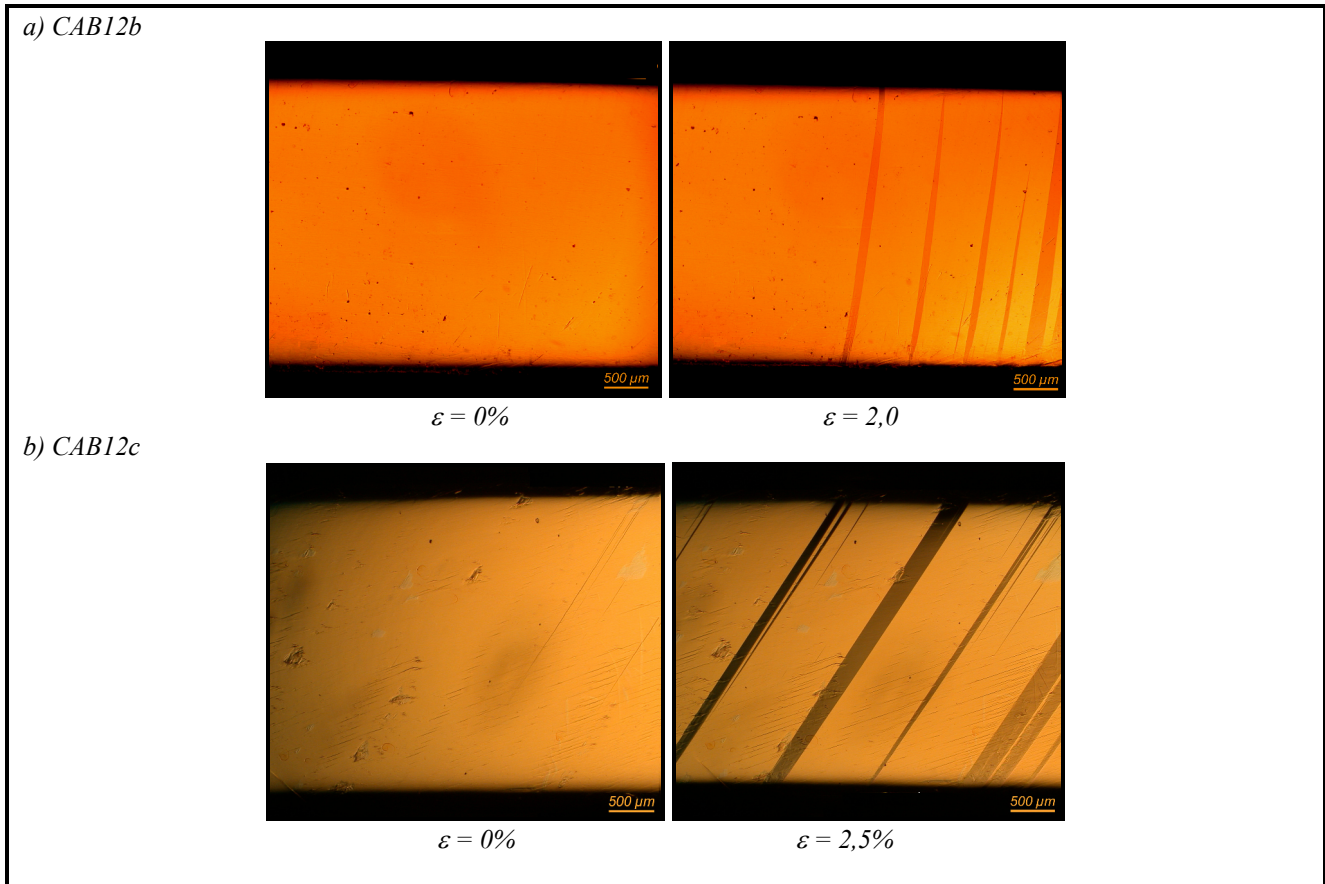


Figure 8. Micrographs of variant induced by stress (martensite plates) with different tensile axis in Cu-Al-Be tensile samples: a) CAB12b – 0 and 2%; b) CAB12c – 0 and 2,5%.

Each martensite single variant produced in the figures 6 and 7 present characteristics different of the properties measured. Table B summarizes the results obtained by tests in the two series of the Cu-Zn-Al and Cu-Al-Be alloys, including critical induction stress, electric resistivity to formation of the martensite single variant and their respective proportionality rates ( $p$ ) and strain transformation ( $\epsilon_{tr}$ ). These results make in evidence the character anisotropic of the martensitic structure. Electric resistivity changes of the martensite single variant reveal dependence with the direction of measure. Centred cubic austenite structure ( $\beta_1$ ) doesn't present electrical anisotropy but the registered variations in each martensite activated variant with some chemical composition must be attributed to the martensite crystal electrical anisotropy (Gonzalez et al, 2001).

Table B. Results of the crystallographic orientations different superelastic tests in the CZA10 and CAB12 samples.

Alloy	CZA10			CAB12		
	a	b	c	a	b	c
Critical Induction Stress - $\sigma_{cr}$ (MPa)	142	128	109	153	123	112
Transformation Strain - $\epsilon_{tr}$ (%)	5.1	5.9	6.8	2.9	5.3	7.2
RE Slope - $p$	7.4	6.6	6.1	9.8	7.1	6.4
ER change - $\Delta\rho_{\epsilon}/\rho_{\epsilon_0}$ (%)	36	39	42	30	44	50

#### 4. CONCLUSIONS

In this work was realized a study of the electromechanical properties behaviour during superelastic tests conducted in single crystals of shape memory alloys under distinct conditions such as: different temperatures tests, different strain rates, submitted to successive martensitic transformations and different crystallographic orientations related to the tensile axis. Mechanical behaviour results were compared with those obtained by the ER variation tests and with others obtained in literature. Summarizing, coupled stress-strain with electrical resistivity measuring in the superelastic tests showed that ER variations depend directly on the induced martensite quantity, independent on temperature and without hysteresis. In the different strain rate tests can introduce a hysteresis loop in the ER curve since the reactions aren't adiabatic. But ER curves are affected by the mechanisms which interfere in the displacement (or pinning) of the austenite/martensite interface during martensitic transformation, for example in pinning (blocking) of interface by quenched supersaturated vacancies (Cingolani et al, 1999). ER curves show different measures and slopes for each martensite type in the successive transformation tests. In the different crystallographic orientations tests was demonstrated martensite single variant anisotropy, in this case independent on chemical composition for each  $\beta_1$ ' martensite variant. These coupled tests results indicate the susceptibility of the electrical resistivity measure in the studies and developments of shape memory effect and martensitic transformation.

#### 5. ACKNOWLEDGEMENTS

Authors wish to thank the supporting and development agencies: Coordenação de Aperfeiçoamento de Pessoal de Nível Superior (CAPES), Conselho Nacional de Desenvolvimento Científico e Tecnológico (CNPq), Fundação de Amparo a Ciência e a Tecnologia do Estado de Pernambuco (FACEPE) by the financial support and the research dissert fellowship. Authors wish to thank Dr. Michel Morin and Dr. Gérard Guénin and at last the Institut National des Sciences Appliquées (INSA) Laboratories, France.

#### 6. REFERENCES

- Amengual, A., Lovey, F.C., Torra, V. – "The hysteretic behaviour of a single-interface martensitic transformation in Cu-Zn-Al shape memory alloys" - Scripta Metallurgica et Materialia, vol. 24, p. 2241-2246, 1990.
- Brown, L.C. – "The thermal effect in pseudoelastic single crystal of  $\beta$ -CuZnSn" – Metallurgical Transactions A, vol. 12A, p. 1491-1494, 1981.
- Brown, L.C. – "The thermal effect in pseudoelastic single crystal of  $\beta$ -CuZnSn" – Metallurgical Transactions A, 1981, vol. 12A, p. 1491-1494.
- Cingolani, E., Stalmans, R., Van Humbeeck, J., Ahlers, M. – "Influence of thermal treatments on the long range order and the two way shape memory effect induced by stabilization in Cu-Al-Be single crystals" – Materials Science and Engineering, vol. A268, p. 109-115, 1999.
- Delaey, L., Ortin, J., Van Humbeeck, J. – "Hysteresis effects in martensitic non-ferrous alloys" - Proceedings of the Phase Transformations 87, London, p. 60-66, 1987.
- Gonzalez, C.H., Araújo, C.J., Quadros, N.F., Guénin, G., Morin, M. – "Study of martensitic stabilisation under stress in Cu-Al-Be shape memory alloy single crystal", Materials Science and Engineering, A 378, p. 253-256, 2004.
- Gonzalez, C.H., Morin, M., Guénin, G. - "Behaviour of electrical resistivity in single crystals of Cu-Zn-Al and Cu-Al-Be under stress", Journal de Physique IV, vol. 11, p. 167-172, 2001.
- Gonzalez, C.H., Quadros, N.F., Araújo, C.J., Morin M., Guénin, G. – "Coupled stress-strain and electrical resistivity measurements on copper based shape memory single crystals", Materials Research, vol. 7, no. 2, p. 305-311, 2004.
- Lovey, F.C., Isalgue A., Torra V. – "Hysteresis loops in stress induced beta-18R martensite transformation in Cu-Zn-Al" - Acta Metallurgical Mater., vol. 40, n° 12, p. 3389-3394, 1992.
- Otsuka, K., Shimizu, K. – "Pseudoelasticity and shape memory effects in alloys" - International Metals Reviews, vol. 31, n° 3, p. 93-114, 1986.
- Wayman, C.M., Otsuka, K., in "Shape Memory Materials, Cambridge University Press, Cambridge, 1998, 386p.

#### 6. RESPONSIBILITY NOTICE

The authors are the only responsible for the printed material included in this paper.

## **7. RESPONSIBILITY NOTICE**

The authors are the only responsible for the printed material included in this paper.